Six-dimensional quantum dynamics of dissociative chemisorption of H2 on Cu(100)

Kroes, G.J.; Baerends, E.J.; Mowrey, R.C.

published in
Journal of Chemical Physics
1997

DOI (link to publisher)
10.1063/1.474682

document version
Publisher's PDF, also known as Version of record

The influence of surface motion on the direct subsurface absorption of H_2 on Pd(111)

R. A. Olsen
Theoretische Chemie, Vrije Universiteit, De Boelelaan 1083, 1081 HV Amsterdam, The Netherlands

G. J. Kroes
Leiden Institute of Chemistry, Gorlaeus Laboratories, Postbus 9502, 2300 RA Leiden, The Netherlands

O. M. Løvvik
University of Oslo, Department of Physics, P.O. Box 1048 Blindern, N–0316 Oslo, Norway

E. J. Baerends
Theoretische Chemie, Vrije Universiteit, De Boelelaan 1083, 1081 HV Amsterdam, The Netherlands

(Received 8 July 1997; accepted 25 August 1997)

Based on density functional theory (DFT) within the generalized gradient approximation (GGA) we have calculated a three-dimensional (3D) potential energy surface (PES) for H_2+Pd(111), depending on two hydrogen molecular degrees of freedom and one palladium surface degree of freedom. The PES is then used in 3D quantum mechanical wave packet calculations to investigate the effect of the surface motion on the direct subsurface absorption. We also compare the full 3D calculations to calculations where the surface motion is included through the sudden approximation. The calculations show a large downward shift of the onset energy for direct subsurface absorption upon inclusion of palladium surface motion (from 0.74 eV to 0.40 eV for H_2). The use of the sudden approximation works well at collision energies greater than 1.3 eV (for H_2), but leads to a significant underestimation of the direct subsurface absorption probability at lower energies. [S0021-9606(97)00345-0]

I. INTRODUCTION

Both experimental[1–7] and theoretical[2,3,8–18] studies agree upon the existence of a hydrogen absorption site on the Pd(111) surface being energetically more favorable than the Pd bulk site and located between the first and second metal layer, a so-called subsurface site. Gdowski, Stulen, and Felter[6] further claim that hydrogen can absorb directly into the palladium bulk, without equilibrating in the chemisorption well.

We will use the term direct subsurface absorption to describe the process of a hydrogen molecule dissociating and its atoms penetrating directly into the subsurface sites without equilibrating in the chemisorption wells. This as opposed to the indirect process where the hydrogen molecule dissociates, its atoms equilibrate in the chemisorption wells on the surface and then penetrate into the lattice through thermally assisted diffusion.

An attempt to model this direct process theoretically was made in Ref. 14 by constructing a model PES and performing quantum mechanical wave packet calculations employing this PES. Due to the model character of the PES and the treatment of only two molecular degrees of freedom, no clear conclusion on the possibility of direct subsurface absorption could be drawn. Munn and Clary[17] then used the model PES introduced in Ref. 14 to include an angular degree of freedom for the hydrogen molecule. They found a substantial probability for hydrogen penetrating directly into the subsurface sites even for the smallest incident kinetic energies of the molecule. Again the model character of the PES made it difficult to draw any clear conclusions on the possibility of direct subsurface absorption, but the study demonstrated clearly the importance of including additional degrees of freedom in the PES.

In Ref. 18 a two-dimensional (2D) PES based on DFT within the GGA was introduced for the H_2+Pd(111) system. The PES had a large barrier to subsurface absorption, and the quantum mechanical wave packet calculations therefore showed no subsurface penetration for a H_2 molecule in its ground vibrational state until the incident kinetic energy of the molecule reached about 0.75 eV. But the calculations also showed that the barrier was strongly dependent on a given displacement of the palladium surface atoms, as also suggested by earlier studies.[9,11,15,16]

In calculations on H_2 dissociation on metal surfaces one often makes the assumption that the metal surface can be treated as static. This assumption is justified by suggesting that the mass mismatch between the molecule and the surface atoms is too large to allow for an efficient energy transfer, and that the densely packed metal surfaces hinder large surface rearrangements.[19] But if, as suggested by Darling and Holloway,[20] a displacement of the surface atoms leads to a sufficiently large change in the PES, the influence of the surface atoms' motion still can be appreciable. Furthermore, if the timescales of the hydrogen molecule's interaction with the surface and the motion of the surface atoms are comparable, as suggested in Ref. 14, the surface degrees of freedom might need to be given a fully dynamical treatment—it might not be sufficient to include the surface motion in an approximate manner. Finally, it is easy to see that treating the surface motion could be of special importance to direct subsur-

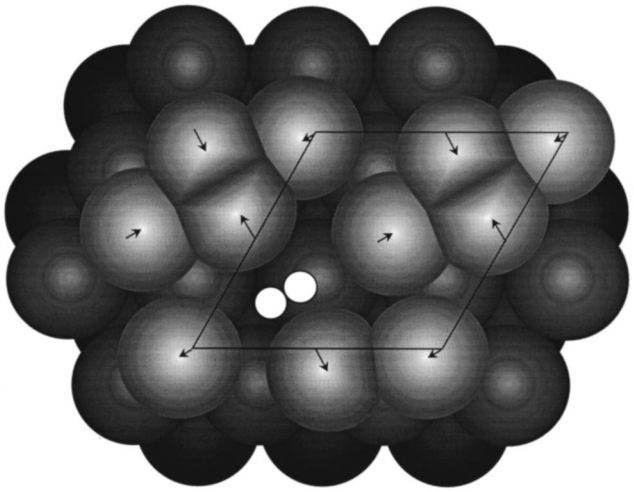

FIG. 1. The palladium atoms constituting the slab used in the calculations of the PES are shown. The 2×2 surface unit cell is marked by the solid lines. The two small white discs represent the hydrogen atoms. The arrows indicate how the palladium atoms in the topmost layer have been displaced from their equilibrium positions. The displacements of the atoms in the figure is exaggerated for clarity.

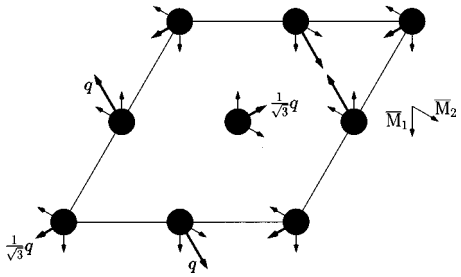

FIG. 2. The palladium atoms in the topmost layer are shown. The 2×2 surface unit cell is marked by the solid lines. The two thin arrows on each palladium atom indicate the displacements belonging to each of the two longitudinal polarized $\bar{M}$ surface phonons. The displacement resulting from the superposition of these two phonons are indicated by the thick arrows. The two phonon wave vectors, $\bar{M}_1$ and $\bar{M}_2$, are also shown (not drawn to scale) with an angle of 60 degrees between them.

face absorption: In this case the dissociating molecule has to move through the first surface layer, which process can be made easier by allowing surface motion so that surface atoms can get out of the molecule's way.

The above considerations have motivated our present study, where we present a 3D PES based on DFT within the GGA, including two hydrogen molecular degrees of freedom and one palladium surface degree of freedom. The PES is employed in quantum mechanical wave packet calculations, and the effect of the surface degree of freedom on the direct subsurface absorption is investigated in full 3D dynamical calculations. For comparison, we will also show results of applying the sudden approximation to the surface degree of freedom. The sudden approximation to surface motion has in earlier studies been applied to the diffractive and phonon-inelastic scattering of a light atom from a surface,[21] and to rotationally and diffractionally inelastic molecule-surface scattering.[22] Here we show how to apply the method to obtain the direct subsurface absorption probability. In making the comparison between the full 3D results and the results of the sudden approximation, we also consider the timescales associated with the different motions taking place during the molecule's encounter with the Pd(111) surface.

The paper is organized as follows. In Sec. II we describe the new 3D PES and in Sec. III we discuss the techniques used in the quantum mechanical wave packet calculations. The results of these calculations are presented in Sec. IV, and Sec. V concludes.

II. THE DFT PES CALCULATIONS

The electronic structure calculations were performed using BAND.[23–25] The hydrogen molecule was adsorbed/absorbed within a 2×2 surface unit cell on one side of a 3 layer slab as shown in Fig. 1. The same basis set and computational parameters as in Ref. 18 were used. For a more complete description of the method and a discussion of approximations and convergence we refer to Ref. 18. Here we only restate the conclusion: The energies constituting the PES should be converged to within 0.1 eV of the GGA limit for the H_2+Pd(111) system. In Ref. 18 it was also shown that the GGA PES compared favorably with the experimental known values.

The three degrees of freedom included in our PES are the distance of the molecule's center of mass to the surface, Z, the hydrogen molecule's bond distance, r, and a coordinate describing a displacement of the palladium surface atoms, q. Z is taken positive above the surface and negative below the surface. The center of mass of the hydrogen molecule is always kept above/below the bridge site, and the bond axis is kept parallel to the surface plane. The atoms move from the bridge site towards the threefold hollow sites as indicated in Fig. 1. The displacement pattern of the palladium surface atoms within the 2×2 surface unit cell is also shown in Fig. 1. This corresponds to the lattice vibrating in two single surface phonon modes, both with a wave vector corresponding to the M point in the surface Brillouin zone.[26] They both have a purely longitudinal polarization, and we have restricted the motion to the topmost layer. The wave vectors form an angle of 60 degrees, and the two modes will of course have the same frequency. The superposition of the two longitudinal $\bar{M}$ surface phonons and the resulting displacements are illustrated in Fig. 2.

The motivation for this choice of the palladium surface atoms' displacements is that we want to include a motion of the surface atoms which is favorable for subsurface penetration. Due to computational considerations we would like to describe this motion by one coordinate only and a single frequency. We also believe, however, that this is a reasonable choice. Other studies have shown that some surface phonons are strongly localized to one metal layer,[27–29] so the restriction of complete localization to the topmost layer may be regarded as a reasonable approximation. Rusina *et al.*[27] have also found that there exists a surface mode at the $\bar{M}$ point with a substantial fraction of longitudinal displacements. We conclude that for the purpose of our model study,

the assumption of the existence of a longitudinally polarized M surface phonon completely localized to the topmost layer is reasonable.

Studying two single phonon modes is somewhat questionable, since a real metal surface generally vibrates in a superposition of a large number of phonon modes. What is the most important is however that our results are of physical relevance. We want to find out whether the hydrogen molecule's degrees of freedom and the metal surface degrees of freedom are dynamically coupled. Then the crucial point is that the surface is treated dynamically, and not that we describe the displacements exactly. But, as will be explained in Sec. IV, we also believe that we find the correct qualitative effect of the influence of the surface motion on the direct subsurface absorption probability. In light of this, our model should be well motivated.

The frequency of the surface motion we have chosen can be found in the following manner. From Fig. 2 we can immediately write down the Hamiltonian governing the motion in q for the four Pd atoms in the topmost layer in the 2×2 surface unit cell,

$$\begin{aligned} H &= \tfrac{1}{2}m_{\mathrm{Pd}}(\dot{q}^2+\dot{q}^2+\tfrac{1}{3}\dot{q}^2+\tfrac{1}{3}\dot{q}^2) \\ &\quad + \tfrac{1}{2}m_{\mathrm{Pd}}\omega_0^2(q^2+q^2+\tfrac{1}{3}q^2+\tfrac{1}{3}q^2) \\ &= \frac{1}{2\mu_q}p_q^2+\tfrac{1}{2}\mu_q\omega_0^2q^2, \end{aligned} \tag{1}$$

where $\mu_q=8m_{\mathrm{Pd}}/3$, $p_q=\mu_q\dot{q}$, $\dot{q}=dq/dt$, and m_{Pd} is the mass of the palladium atom. Performing a set of calculations on a bare Pd slab with different values of the displacement q, the potential energy dependence on q, $V_{\mathrm{Pd}}(q)$, can be determined and the angular frequency, ω_0, found from

$$\omega_0^2=\frac{1}{\mu_q}\left.\frac{d^2V_{\mathrm{Pd}}(q)}{dq^2}\right|_{q=0}. \tag{2}$$

This gives the value 27 meV for ω_0 which is quite close to the angular frequency 24 meV corresponding to the Debye temperature of palladium of 274 K[30] and also reasonably close to the value of 20 meV given in Ref. 27 for one of the M surface phonons. As mentioned above, in the displacement of the surface Pd atoms we have allowed only the atoms in the topmost layer to move. This makes the model lattice appear stiffer than the real lattice and it is therefore no surprise that we find a somewhat higher frequency.

We will treat the motion in the surface coordinate, q, within a harmonic approximation. We have tested the approximation on the bare surface, and the anharmonic terms turned out to be very small. Our 3D PES can thus be written as

$$V_{3D}(Z,r,q)=c_0(Z,r)+c_1(Z,r)q+c_2(Z,r)q^2. \tag{3}$$

The 3D PES can therefore be built up from three 2D PESs with different values for the q coordinate. In Ref. 18 a 2D PES with $q_0=0$ ($V_{2D}^{q_0}$) was calculated. For this study we have calculated two additional 2D PESs with $q_1=0.147\ a_0$ ($V_{2D}^{q_1}$) and $q_2=0.294\ a_0$ ($V_{2D}^{q_2}$). The choice of q_1 and q_2 might seem a bit strange at first sight. But they are chosen so that we get as good a description as possible of the barrier region of the PES. Since, as we will see later, the minimum barrier occurs for a value of q of about 0.19 a_0, we have chosen to have one value close to this one and the other two on each side of this value. The expansion coefficients in Eq. (3) are related to the three 2D PESs according to

$$c_0(Z,r)=V_{2D}^{q_0}(Z,r), \tag{4}$$

$$\begin{aligned} c_1(Z,r) &= \frac{q_2}{q_1(q_2-q_1)}[V_{2D}^{q_1}(Z,r)-V_{2D}^{q_0}(Z,r)] \\ &\quad - \frac{q_1}{q_2(q_2-q_1)}[V_{2D}^{q_2}(Z,r)-V_{2D}^{q_0}(Z,r)], \end{aligned} \tag{5}$$

$$\begin{aligned} c_2(Z,r) &= \frac{1}{q_2(q_2-q_1)}[V_{2D}^{q_2}(Z,r)-V_{2D}^{q_0}(Z,r)] \\ &\quad - \frac{1}{q_1(q_2-q_1)}[V_{2D}^{q_1}(Z,r)-V_{2D}^{q_0}(Z,r)]. \end{aligned} \tag{6}$$

Each 2D PES has been fitted to bicubic splines from a set of 66 points as described in Ref. 18.

In Fig. 3 the 2D PESs $V_{2D}^{q_0}$ and $V_{2D}^{q_1}$ are shown. They both show how the hydrogen molecule bond is broken and energy gained when the molecule approaches the Pd(111) surface. A barrier separates the subsurface absorption minimum from the chemisorption minimum. By comparing Figs. 3(a) and 3(b), we see that the influence of the surface motion is appreciable. In Fig. 3(a) the saddle point, or the barrier to subsurface penetration, is located at $Z=-0.2\ a_0$ and $r=3.2\ a_0$ with a value of about 0.9 eV (the energy is given relative to a free hydrogen molecule and a bare Pd slab with $q=0.0$). In Fig. 3(b) the position of the saddle point has not changed by much, $Z=-0.4\ a_0$ and $r=3.2\ a_0$, but the energy has changed to about 0.5 eV. Thus the barrier to direct subsurface absorption has decreased from about 0.9 eV to about 0.5 eV. To see the influence of the surface motion more clearly, we show how the energy varies in the surface coordinate, q, along a reaction path. The reaction path is the minimum energy path from the H_2 gas phase potential to the subsurface absorption minimum. It is described by a coordinate s, and it is depicted in Fig. 3(a). The value $s=0.0$ corresponds to $Z=5.0$ and $r=1.4$, and $s=1.0$ corresponds to $Z=-1.1$ and $r=3.3$. From Fig. 4 we see that for the smaller values of s the minimum energy occurs for $q=0.0$, i.e., when the hydrogen molecule is more than about 3.0 a_0 away from the surface, the surface remains in its free surface equilibrium position. But when the surface is approached and the barrier climbed, the minimum energy shifts towards positive q values. The minimum barrier to subsurface penetration is about 0.45 eV and occurs for a value of the q coordinate of about 0.19 a_0.

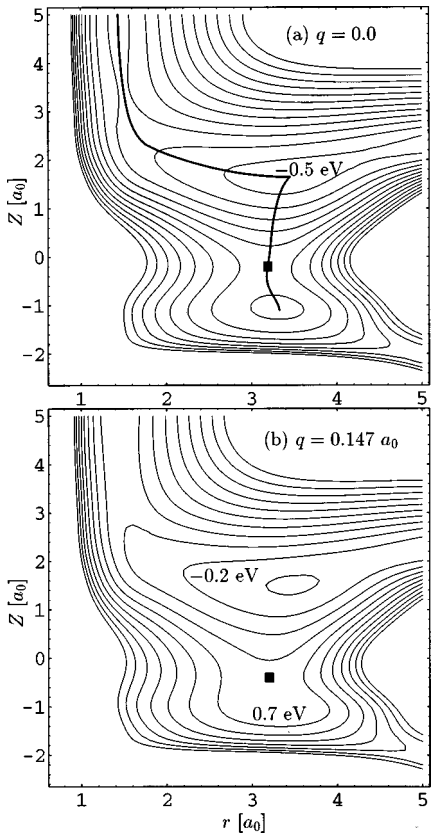

FIG. 3. Contour plots of the two 2D PESs for $q=0.0$ (a) and $q=0.147\ a_0$ (b). The contour spacing is 0.3 eV, and the energies are relative to a free hydrogen molecule and a bare Pd slab with $q=0.0$. The black squares show the position of the saddle points. They have the values 0.9 eV in (a) and 0.5 eV in (b). The first contour line near the bottom of the H_2 gas phase potential is 0.1 eV in (a) and 0.4 eV in (b). In (a) also the reaction path discussed in the text is shown. Z is the hydrogen molecule's center of mass distance to the surface and r the molecule's bond length.

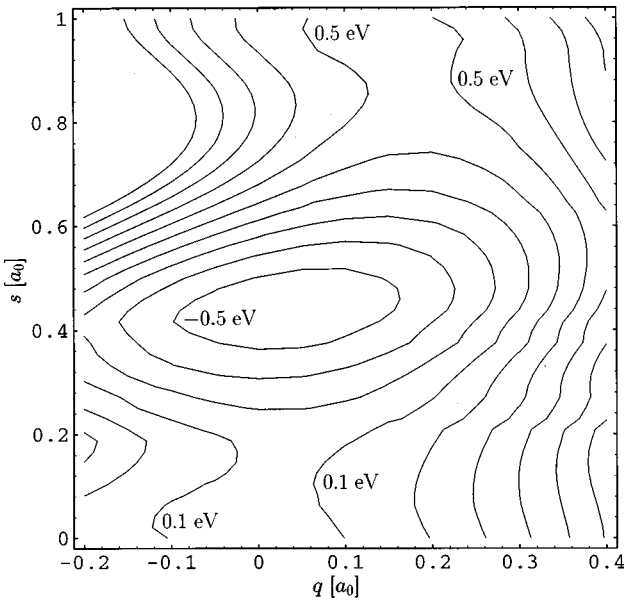

FIG. 4. Contour plot of the energy dependence on the surface coordinate, q, and the reaction path coordinate, s. The contour spacing is 0.2 eV, and the energies are relative to a free hydrogen molecule and a bare Pd slab with $q=0.0$.

III. THE WAVE PACKET CALCULATIONS

The 3D Hamiltonian for our system is given by

$$\hat{H}=-\frac{1}{2M}\frac{\partial^2}{\partial Z^2}-\frac{1}{2\mu}\frac{\partial^2}{\partial r^2}-\frac{1}{2\mu_q}\frac{\partial^2}{\partial q^2}+V(Z,r,q). \quad (7)$$

The hydrogen molecule's total and reduced mass are denoted M and μ, respectively, and μ_q is the mass associated with the surface motion given in the previous section. The interaction potential, $V(Z,r,q)$, will be described later.

To obtain the reaction probabilities, the time-dependent wave packet method is employed. The initial wave function, $\Psi(Z,r,q,t_0)$, is written

$$\Psi(Z,r,q,t_0)=\chi_\nu(r)\phi_{\nu_q}(q)\int dk_z b(k_z) \times\frac{1}{\sqrt{2\pi}}\exp(ik_zZ), \quad (8)$$

where $\chi_\nu(r)$ is a vibrational eigenfunction of the hydrogen molecule labelled by the quantum number ν, $\phi_{\nu_q}(q)$ is a harmonic oscillator eigenfunction for the surface motion labelled by the quantum number ν_q, and $b(k_z)$ is the momentum distribution function for motion in Z given by

$$b(k_z)=\left(\frac{2\zeta^2}{\pi}\right)^{1/4}\exp[-(k_{z_0}-k_z)^2\zeta^2+i(k_{z_0}-k_z)Z_0]. \quad (9)$$

This gives an initial wave function centered on Z_0 with k_{z_0} being its average translational momentum in the Z direction and ζ determining the width of the momentum distribution. The time evolution of the wave function is then obtained by acting with the time evolution operator, $e^{-i\hat{H}t}$, on the initial wave function through the use of the Chebyshev technique.[31]

The wave function is represented on a grid with equally spaced gridpoints spanning the region $-6.0<Z<18.0\ a_0$ and $0.2<r<9.2\ a_0$ with 240 and 60 points in the Z and r directions, respectively. For the q coordinate we use a discrete variable representation (DVR) based on a Gauss–Hermite quadrature rule.[32,33] Convergence of the results was achieved by taking the number of Gauss–Hermite points equal to the number of all open channels. Both the Fourier representation and the gaussian accuracy Gauss–Hermite DVR of the potential energy operator are diagonal in real space.[32–34] Thus the action of the potential energy operator on the wave function can be calculated by multiplying the wave function by the potential energy at each grid/DVR point. The kinetic energy part of the Hamiltonian is found by the fast Fourier transform technique[34,35] for the Z and r coordinates. The kinetic energy part in the q coordinate is found through

$$\frac{\partial^2}{\partial q^2}\Psi(Z,r,q_k)=\left[-\frac{2N_q+1}{3}+\frac{q_k^2}{3}\right]\Psi(Z,r,q_k)+\sum_{\substack{l=1\\ l\neq k}}^{N_q}(-1)^{l+k+1}\frac{2}{(q_k-q_l)^2}\Psi(Z,r,q_l), \tag{10}$$

where N_q is the number of Gauss–Hermite points and q_k and q_l are the Gauss–Hermite quadrature points. It is worth noting that the gaussian accuracy Gauss–Hermite DVR we use differs from the gaussian accuracy Gauss–Hermite DVR used in Ref. 33. The representation used in this study gives harmonic oscillator eigenfunctions equal to the analytical eigenfunctions of the harmonic oscillator in the Gauss–Hermite quadrature points, while the representation used in Ref. 33 does not. However, they are both valid representations connected by the orthogonal transformation matrix $U_{ij}=(-1)^i\delta_{ij}$. As long as one makes sure that the eigenfunctions used correspond to the chosen representation, both representations would yield identical results in the wave packet calculations.

Optical potentials of a quadratic form[36] have been used to absorb the wave packet in the regions $-6.0<Z<-1.1\ a_0$, $12.1<Z<18.0\ a_0$, and $5.0<r<9.2\ a_0$. This avoids artificial reflection from the grid boundaries. A time step of 100 a.u. (2.4 fs) has been used in the Chebyshev expansion to avoid the problem of the Chebyshev expansion being unstable for long propagation steps upon including optical potentials.[37] To keep the grid small in the Z direction the wave packet is brought in on a separate, one-dimensional grid using the projection operator formalism of Neuhauser and Baer.[38]

Analogous to Ref. 18 we analyze the flux through a plane to determine the probability for direct subsurface absorption. The initial state-selected, energy resolved subsurface probability is given by

$$P_{\nu\nu_q}(k_z)=\frac{2\pi}{|k_z|}\,\mathrm{Im}\int dr\,dq\,\Psi^{+*}(k_z|Z_{\mathrm{cut}},r,q)\times\frac{\partial\Psi^{+}}{\partial Z}(k_z|Z,r,q)\bigg|_{Z=Z_{\mathrm{cut}}}, \tag{11}$$

where the stationary scattering states, $\Psi^{+}(k_z|Z,r,q)$, and their derivatives are found from

$$\Psi^{+}(k_z|Z,r,q)=\frac{|k_z|}{2\pi Mb(k_z)}\int_0^{t_{\max}}dt\ \exp(iEt)\times\Psi(Z,r,q,t), \tag{12a}$$

$$\frac{\partial\Psi^{+}}{\partial Z}(k_z|Z,r,q)=\frac{|k_z|}{2\pi Mb(k_z)}\int_0^{t_{\max}}dt\ \exp(iEt)\times\frac{\partial\Psi}{\partial Z}(Z,r,q,t). \tag{12b}$$

The time integrals above are evaluated from the start of the propagation, $t=0$, to a time, $t=t_{\max}$, when the wave function has left the interaction region completely and been absorbed by the optical potentials in the asymptotic regions. We refer to Refs. 18,37,39,40 for a more detailed description of these techniques.

In applying the sudden approximation to the surface motion, we neglect the kinetic energy operator $\partial^2/\partial q^2$ in Eq. (7). We assume that the final subsurface state may be written as $\xi_f(Z,r)\phi_{\nu_q'}(q)$, i.e., that the motion in Z and r on the one hand and the surface motion on the other hand are separable in the final subsurface state, the state associated with the motion of the subsurface dissociated molecule being labelled by the quantum number f. In the sudden approximation, S-matrix elements for a $(\nu\nu_q\rightarrow f\nu_q')$ transition are obtained by calculating

$$S_{\nu\nu_q\rightarrow f\nu_q'}(k_z)=\int dq\,\phi_{\nu_q}^{*}(q)S_{\nu\rightarrow f}(k_z;q)\phi_{\nu_q'}(q)=\langle\phi_{\nu_q}(q)|S_{\nu\rightarrow f}(k_z;q)|\phi_{\nu_q'}(q)\rangle, \tag{13}$$

where $S_{\nu\rightarrow f}(k_z;q)$ are the S-matrix elements obtained from 2D calculations using the Hamiltonian

$$\hat{H}=-\frac{1}{2M}\frac{\partial^2}{\partial Z^2}-\frac{1}{2\mu}\frac{\partial^2}{\partial r^2}+V(Z,r;q). \tag{14}$$

The use of Eq. (13) to obtain the probabilities $P_{\nu\nu_q\rightarrow f\nu_q'}(k_z)$ requires one to work with a formalism designed to obtain S-matrix elements. However, initial state selective probabilities which are summed over the final surface vibrational state, ν_q', may be obtained directly from probabilities using

$$\begin{aligned}P_{\nu\nu_q\rightarrow f}(k_z)&=\sum_{\nu_q'}\langle\phi_{\nu_q}(q)|S_{\nu\rightarrow f}(k_z;q)|\phi_{\nu_q'}(q)\rangle\times\langle\phi_{\nu_q'}(q)|S_{\nu\rightarrow f}^{*}(k_z;q)|\phi_{\nu_q}(q)\rangle\\&=\langle\phi_{\nu_q}(q)||S_{\nu\rightarrow f}(k_z;q)|^2|\phi_{\nu_q}(q)\rangle\\&=\langle\phi_{\nu_q}(q)|P_{\nu\rightarrow f}(k_z;q)|\phi_{\nu_q}(q)\rangle,\end{aligned} \tag{15}$$

where we have used the completeness relation for the surface vibrational states. It is then trivial to show that the initial state dependent subsurface reaction probability is given, in the sudden approximation, by

$$P_{\nu\nu_q}(k_z)=\langle\phi_{\nu_q}(q)|P_{\nu}(k_z;q)|\phi_{\nu_q}(q)\rangle, \tag{16}$$

where

$$P_{\nu}(k_z;q)=\sum_f P_{\nu\rightarrow f}(k_z;q). \tag{17}$$

In this paper we do not compute individual reaction probabilities $P_{\nu\rightarrow f}(k_z;q)$ to obtain the initial state-selected reaction probability by summation. Rather, $P_{\nu}(k_z;q)$ is obtained directly by performing 2D calculations using the flux-formalism above for obtaining initial state-selected reaction probabilities,

$$P_\nu(k_z;q)=\frac{2\pi}{|k_z|}\,\mathrm{Im}\int dr\Psi^{+*}(k_z|Z_{\mathrm{cut}},r;q)\times\frac{\partial\Psi^{+}}{\partial Z}(k_z|Z,r;q)\Big|_{Z=Z_{\mathrm{cut}}}, \tag{18}$$

for a number of different Gauss–Hermite quadrature points in q. After this, application of Eq. (16) yields the direct subsurface absorption probability in the sudden approximation.

The PES in Eq. (3) has not been calculated for $Z>5.0\ a_0$. But by using a switching function to append the H_2 gas phase potential, $V_{H_2}(r)$, and the free surface potential, $V_{\mathrm{Pd}}(q)$, to this PES, we make sure the interaction potential, $V(Z,r,q)$, needed in Eq. (7) is defined also for Z larger than 5.0 a_0:

$$\begin{aligned}
&V(Z,r,q)=V_{3\mathrm{D}}(Z,r,q), \quad Z\leqslant 5.0a_0,\\
&V(Z,r,q)=f_{\mathrm{switch}}(Z)V_{3\mathrm{D}}(5.0a_0,r,q)+[1-f_{\mathrm{switch}}(Z)]\\
&\qquad\times[V_{H_2}(r)+V_{\mathrm{Pd}}(q)],\\
&\qquad 5.0a_0<Z<6.75a_0,\\
&V(Z,r,q)=V_{H_2}(r)+V_{\mathrm{Pd}}(q), \quad Z\geqslant 6.75a_0.
\end{aligned} \tag{19}$$

The switching function is given by

$$f_{\mathrm{switch}}(Z)=\frac{1}{2}+\frac{1}{2}\cos(\chi), \quad \chi=\frac{(Z-5.0a_0)\pi}{1.75a_0}. \tag{20}$$

Furthermore, the PES is set equal to its value on the plane $Z=-1.1\ a_0$ for all planes with $Z<-1.1\ a_0$. This then constitutes the interaction potential, $V(Z,r,q)$, in Eq. (7). More comments can be found in Ref. 18.

IV. RESULTS

Results for the direct subsurface absorption probability of $\nu=0$ H_2 (D_2) with the surface in the initial $\nu_q=0$ state are shown in Fig. 5. Results for a static surface are also shown. There are some important effects on the probability for direct subsurface absorption when including Pd surface motion. For H_2 (D_2) the onset of direct subsurface penetration is shifted down from 0.74 eV (0.79 eV) to 0.40 eV (0.48 eV). We also see that the curve for direct subsurface penetration becomes a lot smoother upon including surface motion, i.e., the presence of resonance structures is appreciably reduced. But, disregarding the structure in the static result, we also see that the curve for the static surface follows the curve including surface motion quite closely for the higher energies.

The energy dependence of $P_{00}(k_z)$ as obtained with the sudden approximation by the used of 21 Gauss-Hermite points in Eq. (16) is compared to the exact results in Fig. 6. The sudden approximation seems to perform quite well at first glance. But a closer look at the low energy regime for the H_2 (D_2) curve reveals important differences. For the full 3D calculation the onset of direct subsurface absorption occurs around 0.40 eV (0.48 eV). In the sudden approximation the onset lies at about 0.55 eV (0.63 eV). Thus the sudden

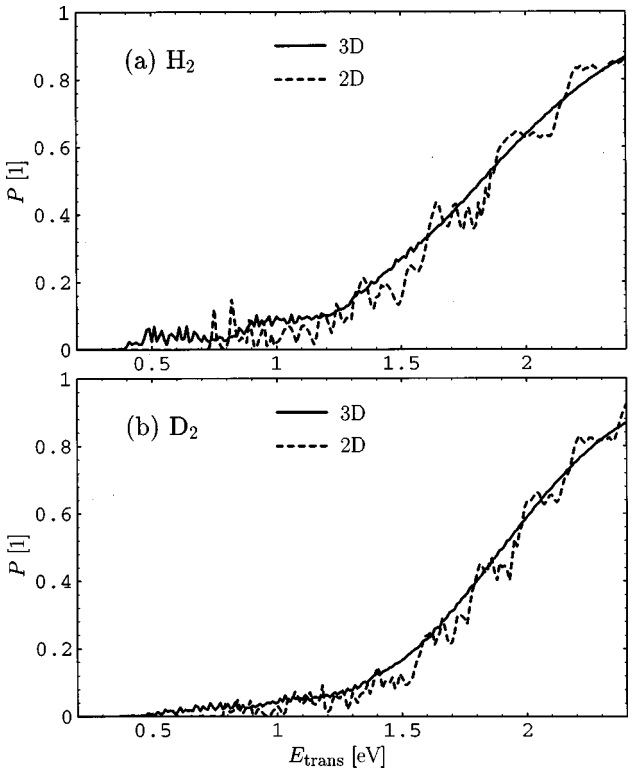

FIG. 5. The probability for direct subsurface absorption (P) for H_2 and D_2 initially in their ground vibrational state for different initial translational energies (E_{trans}). Results for a static surface (2D) and a surface initially in its ground vibrational state (3D) are given.

approximation does not describe the low energy tail of the direct subsurface absorption curve well. At higher energies, however, the agreement is better.

To help interpret the results in Figs. 5 and 6 we have performed a full 3D calculation (with the maximum value of Z allowed on the grid increased to 36.0 a_0) on an initial wave packet centered on a translational energy of about 0.52 eV with a narrow distribution in energies. In Fig. 7 we have plotted the expectation value of the kinetic energy in the q coordinate ($\langle K_q\rangle$), the expectation value of the q coordinate ($\langle q\rangle$), and the expectation value of the Z coordinate, the hydrogen molecule's center of mass distance to the surface ($\langle Z\rangle$). We see that the hydrogen (deuterium) molecule spends a time of about 2000 a.u. (2500 a.u.) closer than 3.0 a_0 from the surface. During this time a bit of the wave packet penetrates the subsurface region and is absorbed by an optical potential. Another part of the wave packet leaves through the surface channel and is also absorbed by an optical potential, i.e., the hydrogen (deuterium) molecule dissociatively adsorbs on the surface. The rest of the wave packet is scattered back towards the entrance channel. Figure 7 clearly shows how energy is transferred from the molecule to the surface during the encounter and that the transferred energy remains in the surface coordinate after the collision. The result for the expectation value of q indicates that the wave packet is steered in the direction of the minimum barrier, which occurs for an extended value of q as discussed in Sec. II. Or stated differently, the incoming molecule pushes the

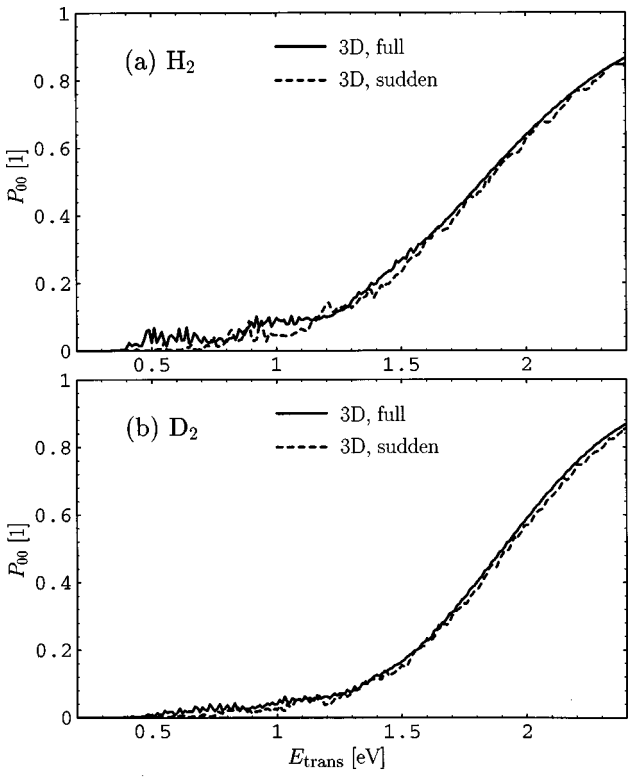

FIG. 6. The probability for direct subsurface absorption (P_{00}) for H_2 and D_2 initially in their ground vibrational state for different initial translational energies (E_{trans}). Results for a full 3D treatment and the sudden approximation are given. The surface is initially in its ground vibrational state.

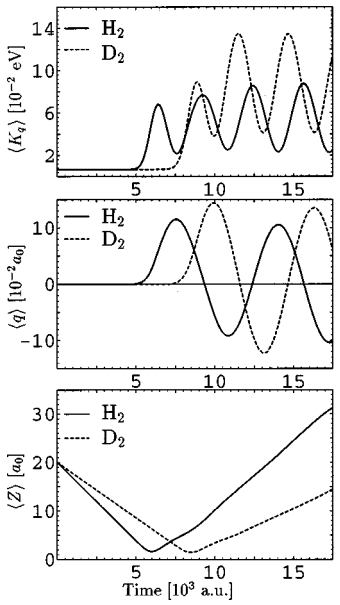

FIG. 7. The expectation value of the kinetic energy in the q coordinate ($\langle K_q \rangle$), the expectation value of the q coordinate ($\langle q \rangle$), and the expectation value of the Z coordinate ($\langle Z \rangle$) are given as function of time. The initial wave packet is centered on a translational energy of about 0.52 eV and has a narrow distribution in energies. Both the molecule and the surface are initially in their ground vibrational states.

palladium atoms away from their equilibrium positions, and this leads to the hydrogen atoms seeing a reduced barrier to subsurface penetration. The steering is the reason for the 0.34 eV (0.31 eV) downshift in the onset of direct subsurface absorption seen in Fig. 5 for H_2 (D_2). Thus we see that the collision time of about 2000 a.u. (2500 a.u.) for H_2 (D_2) is long enough compared to the timescale of the surface motion of about 6400 a.u. ($2\pi/\omega_0$) for an efficient steering to take place. However, the motion in the q coordinate does not completely follow the minimum energy path to the subsurface region—if it had done so the downshift in the onset of direct subsurface absorption would have been about equal to the reduction in the barrier of about 0.45 eV. As discussed in Sec. II the minimum barrier occurs for a value of q of about 0.19 a_0. From Fig. 7 we see that during the collision the expectation value of q does not exceed about 0.12 a_0 (0.15 a_0), and the minimum barrier is not reached, i.e., the steering is not strong enough to let the wave packet follow the minimum energy path to the subsurface region.

The observed steering also explains why the sudden approximation does not do so well for the low energies. The steering of the wave packet towards the minimum barrier means that neglecting the kinetic energy operator in q, $\partial^2/\partial q^2$, is too crude an approximation. Thus for low incident kinetic energies the surface and molecular degrees of freedom are dynamically coupled. Increasing the incident kinetic energy shortens the collision time, and the steering is no longer so efficient. Again stated differently, the hydrogen molecule does not manage to push the palladium atoms far enough away from their equilibrium position for the hydrogen atoms to experience a reduced barrier. The sudden approximation therefore works better.

As mentioned in Sec. II, and also pointed out by the referee, we are only treating one out of many possible surface modes. Although our model clearly shows that the chosen mode is dynamically coupled to the molecular degrees of freedom in the low energy regime, it is not evident that this single mode will predict the correct qualitative effect of a general surface motion on the direct subsurface absorption probability. In Ref. 41 it was shown that the surface motion reduces (as compared to a model where the nickel atoms are not allowed to move) the resurfacing rate of hydrogen placed in subsurface sites on Ni(111), and Yang and Rabitz[42] found that surface motion had minimal effect on the penetration of energetic hydrogen atoms on a Pd(100) surface. But we believe that the enhanced subsurface penetration at lower energies seen in our single mode model is qualitatively correct and would still be seen if the model included a more complete description of the surface motion. The reason is as follows: In Sec. II we saw that the PES was strongly dependent on the positions of the surface atoms. The motion of the surface atoms according to the mode we have chosen, is probably one which yields the largest decrease (and increase) of the barrier. All other surface motions would probably give a smaller energetic variation of the barrier. Thus a PES including all possible surface modes is likely to show the strongest energetic variation along the mode we have chosen. As explained above, the downshift in the onset of direct subsurface absorption seen in Fig. 5, is caused by steering along

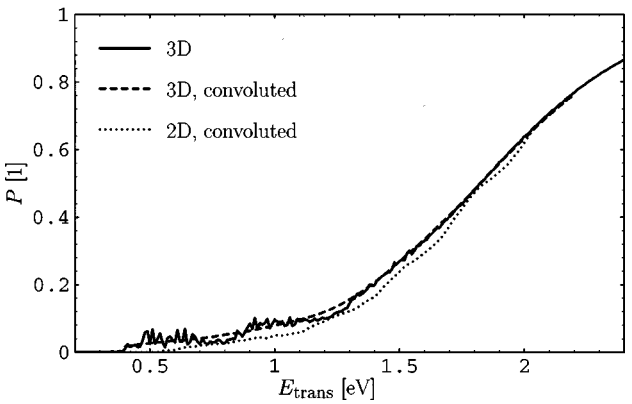

FIG. 8. The convolution of the curves in Fig. 5(a) is shown, using Eqs. (21) and (22) (see text).

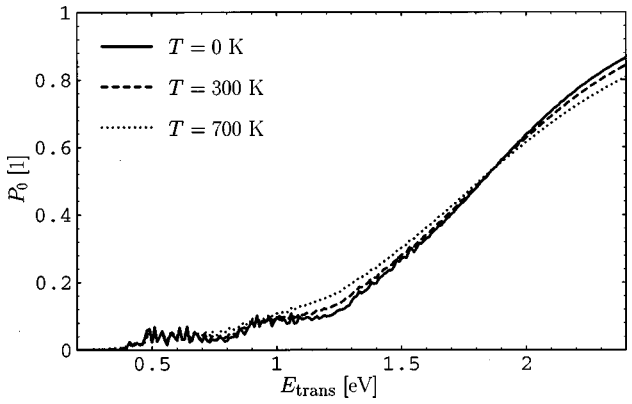

FIG. 9. The probability for direct subsurface absorption (P_0) for H_2 initially in its ground vibrational state for different initial translational energies (E_{trans}). Results for three different temperatures (T) are given.

the surface coordinate. On a multi-dimensional PES including all surface modes, the wave packet can be expected to be steered in the direction of the largest decrease in potential energy, i.e., in the direction described by our chosen mode. Stated a bit differently, the interaction between the surface modes and the molecular degrees of freedom is dominated by the mode we have chosen. Although the other modes will influence the results quantitatively, we do not think they will change them qualitatively.

Returning briefly to Fig. 5(a), it looks like the 3D curve is a bit shifted towards lower energies when compared to the 2D curve. To see this more clearly we have convoluted the curves by using the simple convolution

$$P_{\text{conv}}(E_{\text{trans}}) = \int dE f(E;E_{\text{trans}}) P(E), \tag{21}$$

where

$$f(E;E_{\text{trans}}) = \begin{cases} \dfrac{1}{2\Delta E} & E_{\text{trans}} - \Delta E < E < E_{\text{trans}} + \Delta E \\ 0 & \text{otherwise} \end{cases} \tag{22}$$

with $\Delta E = 0.2$ eV. The results are shown in Fig. 8. As seen, at energies lower than 2 eV the 3D curve is always above the 2D curve.

As in Ref. 43 we simulate the effect of a finite surface temperature, T, through

$$P_\nu(k_z,T) = \sum_{\nu_q} w_{\nu_q} P_{\nu\nu_q}(k_z), \tag{23}$$

where

$$w_{\nu_q} = \frac{e^{-\nu_q \omega_0/kT}}{\Sigma_{\nu_q} e^{-\nu_q \omega_0/kT}}. \tag{24}$$

The surface vibrational ground state and the first ten excited states have been used in the above formulas to converge the results up to a temperature of 700 K. There are three things to note from the results in Fig. 9. The onset of the direct subsurface absorption does not depend on the temperature. It remains at about 0.40 eV for the temperatures shown. However, for energies larger than about 1.0 eV we do see a broadening of the reaction curve upon increasing the temperature. And finally the results suggest that there is an isoprobabilistic point at an energy of about 1.85 eV in the three curves.

In Ref. 43 Dohle and Saalfrank used the surface oscillator (SO) model of Hand and Harris,[44] the surface mass (SM) model of Luntz and Harris,[45] and their own modified surface oscillator (MSO) model to study the effect of the surface temperature on the dissociative adsorption of H_2 on a Cu model surface. Although we are treating a different problem [direct subsurface absorption of H_2 on Pd(111)], it is interesting to consider the similarities as well as the differences found for the influence of surface motion on dissociative adsorption and direct subsurface absorption.

In direct subsurface absorption, we find that heating the surface does not promote reaction in the low energy onset regime. This is in contrast to dissociative adsorption. A possible explanation is that, as discussed above, steering along the surface coordinate is important in the low energy onset regime of direct subsurface absorption. In such a mechanism, it will not be very helpful if the surface atoms move faster initially. In dissociative adsorption, however, the PES can be expected to have a much weaker dependence on the surface coordinate and steering along the surface coordinate should not be as important a mechanism for reaction—therefore a different dependence of the temperature in the low energy onset regime might be expected.

At higher energies, we find a broadening of the subsurface reaction probability curve with increasing temperature around an isoprobabilistic point, as is found in all models looking at dissociative adsorption.[43–45] Increasing the surface temperature has thus similar effects on dissociative adsorption and direct subsurface absorption: At low collision energies, exciting the phonon motion helps the molecule to overcome the barrier to reaction, whereas at high collision energies exciting the phonon motion inhibits the reaction.

Finally, as noted above for direct subsurface absorption, the 3D reaction probability curve is on average above the 2D curve, as shown most clearly in Fig. 8. Thus, surface motion promotes direct subsurface absorption. In this respect, direct

subsurface absorption is similar to dissociative adsorption as viewed in the MSO model of Dohle and Saalfrank,[43] but different from dissociative adsorption in the SO[44] and SM[45] models. In the MSO model, the reaction probability curve shifts to lower energies upon inclusion of surface motion, whereas an upward shift is found for the SO and SM models. The similar behavior of the direct subsurface absorption probability and the dissociative adsorption probability in the MSO model is easily understood: In the MSO model, the reaction barrier height is allowed to vary with the phonon coordinate, as is also the case for the PES we have used here to model direct subsurface absorption. In contrast, the SO and SM models only make the location of the barrier dependent on the phonon coordinate.

V. CONCLUSIONS

We have used density functional theory within the generalized gradient approximation to calculate a three-dimensional (3D) potential energy surface (PES) for H_2+Pd(111), describing two hydrogen molecular degrees of freedom and one palladium surface degree of freedom. The PES is strongly dependent on the surface coordinate. The minimum barrier to subsurface penetration is reduced from about 0.9 eV for a static surface to about 0.45 eV when Pd surface motion is included.

Full 3D quantum mechanical calculations were performed on the PES and compared to calculations treating the Pd surface motion in a sudden approximation. These calculations showed that at collision energies lower than about 1.0–1.1 eV the strong dependence of the PES on the surface coordinate leads to a steering of the wave packet along this surface coordinate towards the minimum barrier. Thus the onset of direct subsurface absorption was shifted down by as much as 0.34 eV (0.31 eV) for the H_2 (D_2) molecule when comparing calculations including palladium surface motion and calculations on a static Pd(111) surface. The efficient steering at low energies could be understood by looking at the timescales—compared to the phonon vibrational period, the collision time is long enough for the wave packet to be steered in the direction of the minimum barrier (along the phonon coordinate). This also explained the breakdown of the sudden approximation for the low energies—the molecular and surface degrees of freedom are dynamically coupled in the low energy regime.

We also saw how the sudden approximation performed quite well for the higher energies ($E>1.3$ eV for H_2, $E>1.1$ eV for D_2) or shorter collision times. For the higher energies the steering is no longer so efficient, and the molecular and surface degrees of freedom can be decoupled through the sudden approximation.

Furthermore, in simulating the effect of a surface at finite temperature, we found a thermal broadening of the direct subsurface absorption probability curve and an isoprobabilistic point. The onset of direct subsurface absorption was found to be independent of the temperature. We further found that allowing surface motion at 0 K promotes direct subsurface absorption, as is also found for dissociative adsorption in the modified surface oscillator model of Dohle and Saalfrank[43] in which the barrier height to dissociation is allowed to vary with a phonon coordinate.

We conclude that, for computing the direct subsurface absorption probability of H_2+Pd(111), it is important to include the effect of the surface motion. In the low collision energy regime the palladium surface motion must be given a full dynamical treatment—the molecular and surface degrees of freedom are dynamically coupled. However, in the high energy regime, the surface motion can be included through the sudden approximation.

ACKNOWLEDGMENTS

The calculations reported here have been carried out under a grant of computer time by the Dutch National Computing Facilities Foundation (NCF). Both R.A.O. and O.M.L. are financed by the Norwegian Research Council. G.J.K. acknowledges financial support by the Royal Netherlands Academy of Arts and Sciences (KNAW).

[1] W. Eberhardt, F. Greuter, and E. W. Plummer, Phys. Rev. Lett. **46**, 1085 (1981).
[2] W. Eberhardt, S. G. Louie, and E. W. Plummer, Phys. Rev. B **28**, 465 (1983).
[3] T. E. Felter, S. M. Foiles, M. S. Daw, and R. H. Stulen, Surf. Sci. Lett. **171**, L379 (1986).
[4] G. D. Kubiak and R. H. Stulen, J. Vac. Sci. Technol. A **4**, 1427 (1986).
[5] G. E. Gdowski, T. E. Felter, and R. H. Stulen, Surf. Sci. Lett. **181**, L147 (1987).
[6] G. E. Gdowski, R. H. Stulen, and T. E. Felter, J. Vac. Sci. Technol. A **5**, 1103 (1987).
[7] T. E. Felter, E. C. Sowa, and M. A. van Hove, Phys. Rev. B **40**, 891 (1989).
[8] C. T. Chan and S. G. Louie, Phys. Rev. B **30**, 4153 (1984).
[9] M. S. Daw and S. M. Foiles, Phys. Rev. B **35**, 2128 (1987).
[10] D. L. Lynch, S. W. Rick, M. A. Gomez, B. W. Spath, J. D. Doll, and L. R. Pratt, J. Chem. Phys. **97**, 5177 (1992).
[11] S. W. Rick, D. L. Lynch, and J. D. Doll, J. Chem. Phys. **99**, 8183 (1993).
[12] J. Rogan, M. Lagos, and I. K. Schuller, Surf. Sci. Lett. **318**, L1165 (1994).
[13] R. Löber, Ph.D. thesis, Humboldt-University of Berlin, 1995.
[14] O. M. Løvvik and R. A. Olsen, J. Chem. Phys. **104**, 4330 (1996).
[15] J. F. Paul and P. Sautet, Phys. Rev. B **53**, 8015 (1996).
[16] R. Löber and D. Hennig, Phys. Rev. B **55**, 4761 (1997).
[17] N. S. Munn and D. C. Clary, Chem. Phys. Lett. **266**, 437 (1997).
[18] R. A. Olsen, P. H. T. Phlipsen, E. J. Baerends, G. J. Kroes, and O. M. Løvvik, J. Chem. Phys. **106**, 9286 (1997).
[19] A. Gross, Surf. Sci. **363**, 1 (1996).
[20] G. R. Darling and S. Holloway, Surf. Sci. Lett. **321**, L189 (1994).
[21] J. E. Adams and W. H. Miller, Surf. Sci. **85**, 77 (1979).
[22] R. Schinke and R. B. Gerber, J. Chem. Phys. **82**, 1567 (1985).
[23] G. te Velde, Ph.D. thesis, Vrije Universiteit, Amsterdam, 1990.
[24] G. te Velde and E. J. Baerends, Phys. Rev. B **44**, 7888 (1991).
[25] http://tc.chem.vu.nl/SCM/Doc/BANDUG/BANDUG.html.
[26] F. W. de Wette, in *Springer Series in Surface Sciences*, edited by W. Kress and F. W. de Wette (Springer-Verlag, Berlin, 1991), Vol. 21.
[27] G. G. Rusina, I. Y. Sklyadneva, and E. V. Chulkov, Phys. Solid State **38**, 818 (1996).
[28] A. Wachter, K. P. Bohnen, and K. M. Ho, Surf. Sci. **346**, 127 (1996).
[29] A. M. Lahee, J. P. Toennies, and C. Wöll, Surf. Sci. **191**, 529 (1987).
[30] C. Kittel, *Introduction to Solid State Physics*, 6th ed. (Wiley, New York, 1986).
[31] H. Tal-Ezer and R. Kosloff, J. Chem. Phys. **81**, 3967 (1984).
[32] J. C. Light, I. P. Hamilton, and J. V. Lill, J. Chem. Phys. **82**, 1400 (1985).
[33] V. Szalay, J. Chem. Phys. **99**, 1978 (1993).

[34] D. Kosloff and R. Kosloff, J. Comput. Phys. **52**, 35 (1983).
[35] M. D. Feit, J. A. Fleck, Jr., and A. Steiger, J. Comput. Phys. **47**, 412 (1982).
[36] Á. Vibók and G. G. Balint-Kurti, J. Phys. Chem. **96**, 8712 (1992).
[37] D. Neuhauser, M. Baer, R. S. Judson, and D. J. Kouri, Comput. Phys. Commun. **63**, 460 (1991).
[38] D. Neuhauser and M. Baer, J. Chem. Phys. **91**, 4651 (1989).
[39] D. H. Zhang and J. Z. H. Zhang, J. Chem. Phys. **101**, 1146 (1994).
[40] R. C. Mowrey and G. J. Kroes, J. Chem. Phys. **103**, 1216 (1995).
[41] R. Baer, Y. Zeiri, and R. Kosloff, Phys. Rev. B **55**, 10 952 (1997).
[42] K. Yang and H. Rabitz, J. Chem. Phys. **101**, 8205 (1994).
[43] M. Dohle and P. Saalfrank, Surf. Sci. **373**, 95 (1997).
[44] M. Hand and J. Harris, J. Chem. Phys. **92**, 7610 (1990).
[45] A. C. Luntz and J. Harris, Surf. Sci. **258**, 397 (1991).